iScience

Article

Mapping the chromothripsis landscape in urothelial carcinoma unravels great intratumoral and intertumoral heterogeneity

Graphical abstract

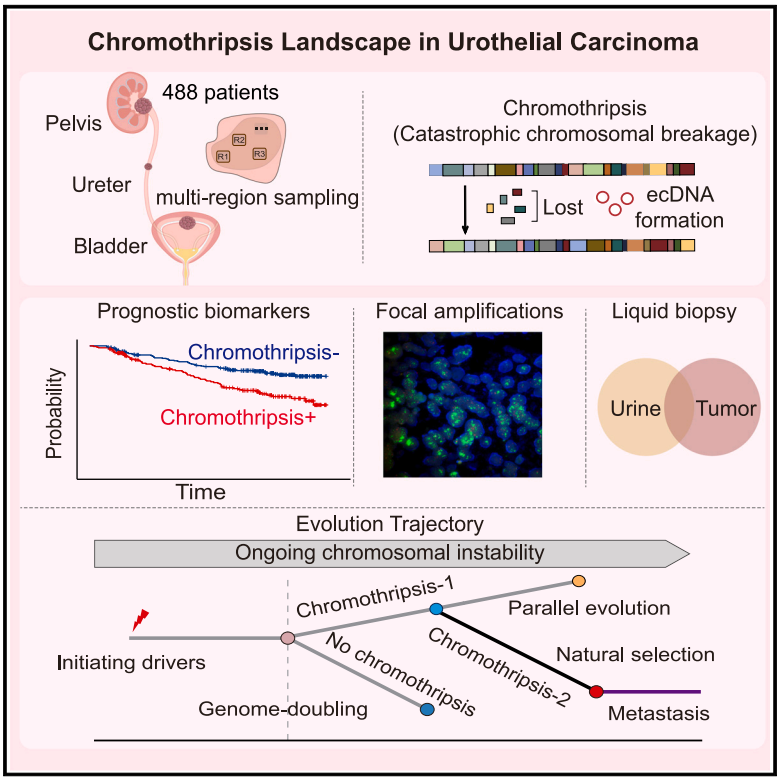

Highlights

- A landscape of chromothripsis in urothelial carcinoma (UC)
- Chromothripsis is highly heterogeneous in UC
- Chromothripsis correlates with UC clinical outcome

Authors

Yuchen Zeng (曾雨晨), Wei Lv (吕伟), Huiying Tao (陶荟颖), ..., Yonglun Luo (罗永伦), Chunhua Lin (林春华), Peng Han (韩鹏)

Correspondence

lvwei@biomed.au.dk (W.L.), songjinzhao@ucas.ac.cn (J.S.), drxchsong@163.com (X.S.), alun@biomed.au.dk (Y.Luo), chunhua.lin@qdu.edu.cn (C.Lin), han.peng@bio.ku.dk (P.H.)

In brief

Genomics; Genomic analysis; Cancer systems biology; Cancer

Zeng et al., 2025, iScience 28, 111510
January 17, 2025
https://doi.org/10.1016/j.isci.2024.111510

CellPress

iScience

CellPress
OPEN ACCESS

Article

Mapping the chromothripsis landscape in urothelial carcinoma unravels great intratumoral and intertumoral heterogeneity

Yuchen Zeng (曾雨晨),[1,2,19] Wei Lv (吕伟),[2,3,4,5,19,*] Huiying Tao (陶荟颖),[6,7,19] Conghui Li (李聪慧),[8,19] Shiqi Jiang (蒋世琪),[1,2] Yuan Liang (梁媛),[9] Chen Chen (陈晨),[2] Tianxi Yu (于天熙),[7] Yue Li (李悦),[7] Shuang Wu (吴双),[7] Xin Cui (崔鑫),[7] Ning Liang (梁宁),[7] Ping Wang (王平),[9] Huixin Xu (许荟馨),[5] Jingjing Dong (董晶晶),[10] Huajing Teng (滕花景),[11] Ke Chen (谌科),[12] Kai Mu (穆锴),[13] Tianda Fan (范天达),[2] Xiaoping Cen (岑萧萍),[2,4] Zhe Xu (许喆),[4] Ming Zhu (朱明),[14] Wenting Wang (王文亭),[7] Jia Mi (米佳),[15] Xi Xiang (向熙),[16] Wei Dong (董伟),[2] Huanming Yang (杨焕明),[2] Lars Bolund,[2] Lin Lin (林琳),[5,18] Jinzhao Song (宋金召),[2,*] Xicheng Song (宋西成),[17,*] Yonglun Luo (罗永伦),[5,18,20,*] Chunhua Lin (林春华),[7,*] and Peng Han (韩鹏)[8,16,*]

[1]School of Life Sciences, Faculty of Medicine, Tianjin University, Tianjin 300072, China
[2]HIM-BGI Omics Center, Hangzhou Institute of Medicine (HIM), Chinese Academy of Sciences, Hangzhou, Zhejiang 310022, China
[3]Department of Urology & Andrology, Sir Run Run Shaw Hospital, Zhejiang University School of Medicine, Hangzhou 310016, China
[4]College of Life Sciences, University of Chinese Academy of Science, Beijing 100049, China
[5]Department of Biomedicine, Aarhus University, 8200 Aarhus, Denmark
[6]The 2nd Medical College of Binzhou Medical University, Yantai, Shandong 264003, China
[7]Department of Urology, The Affiliated Yantai Yuhuangding Hospital of Qingdao University, Yantai, Shandong 264000, China
[8]Department of Biology, University of Copenhagen, 2100 Copenhagen, Denmark
[9]CAS Key Laboratory of Genomic and Precision Medicine, Beijing Institute of Genomics, Chinese Academy of Sciences and China National Center for Bioinformation, Beijing 100101, China
[10]Department of General Medicine, Zhejiang Cancer Hospital, Hangzhou Institute of Medicine (HIM), Chinese Academy of Sciences, Hangzhou, Zhejiang 310022, China
[11]Key Laboratory of Carcinogenesis and Translational Research (Ministry of Education/Beijing), Department of Radiation Oncology, Peking University Cancer Hospital & Institute, Beijing 100142, China
[12]Department of Urology, Tongji Hospital, Tongji Medical College, Huazhong University of Science and Technology, Wuhan 430000, China
[13]The Second Hospital, Cheeloo College of Medicine, Shandong University, Shandong 250033, China
[14]Tsinghua-Peking Joint Center for Life Sciences, Tsinghua University, Beijing 100084, China
[15]Shandong Technology Innovation Center of Molecular Targeting and Intelligent Diagnosis and Treatment, Binzhou Medical University, Yantai, Shandong 264003, China
[16]Scientific Research Center, The Seventh Affiliated Hospital, Sun Yat-Sen University, Shenzhen 518107, Guangdong, China
[17]Department of Otorhinolaryngology, Head and Neck Surgery, The Affiliated Yantai Yuhuangding Hospital of Qingdao University, Yantai, Shandong 264000, China
[18]Steno Diabetes Center Aarhus, Aarhus University Hospital, Aarhus, Denmark
[19]These authors contributed equally
[20]Lead contact
*Correspondence: lvwei@biomed.au.dk (W.L.), songjinzhao@ucas.ac.cn (J.S.), drxchsong@163.com (X.S.), alun@biomed.au.dk (Y.Luo), chunhua.lin@qdu.edu.cn (C.Lin), han.peng@bio.ku.dk (P.H.)
https://doi.org/10.1016/j.isci.2024.111510

SUMMARY

Chromothripsis, a hallmark of cancer, is characterized by extensive and localized DNA rearrangements involving one or a few chromosomes. However, its genome-wide frequency and characteristics in urothelial carcinoma (UC) remain largely unknown. Here, by analyzing single-regional and multi-regional whole-genome sequencing (WGS), we present the chromothripsis blueprint in 488 UC patients. Chromothripsis events exhibit significant intertumoral heterogeneity, being detected in 41% of UC patients, with an increase from 30% in non-muscle-invasive disease (Ta/1) to 53% in muscle-invasive disease (T2-4). The presence of chromothripsis correlates with an unstable cancer genome and poor clinical outcomes. Analysis of multi-regional WGS data from 52 patients revealed pronounced intratumoral heterogeneity with chromothripsis events detectable only in specific tumor regions rather than uniformly across all areas. Chromothripsis events evolve under positive selection and contribute to tumor dissemination. This study presents a comprehensive genome-wide chromothripsis landscape in UC, highlighting the significance of chromothripsis in UC development.

INTRODUCTION

Urothelial carcinoma (UC) is a highly invasive malignancy within the urinary tract. Most UC cases, approximately 90%–95%, originate in the bladder, while tumors located in the renal pelvis and ureter are less common, accounting for 5%–10% of all UCs. Depending on the degree of tumor invasion, UC can be classified into non-muscle-invasive (pTa/1) and muscle-invasive (pT2-T4) subtypes. A long-standing challenge in the clinical management of UC is the absence of effective targeted therapeutic drugs, especially for patients with muscle-invasive disease.[1–3] A comprehensive understanding of the molecular mechanisms underlying the onset of UC is crucial for effectively managing the disease.

Chromosomal instability has been implicated in UC development.[4–6] This instability can lead to chromothripsis, a phenomenon characterized by extensive and localized DNA rearrangements involving one or a few chromosomes.[7–10] This intricate genomic rearrangement mosaic arises from the continuous, inaccurate repair of shattered DNA fragments, leading to the swift accumulation of numerous rearrangements within only a few cell divisions. Chromothripsis has been observed across a wide spectrum of tumor types and is associated with aggressive biological behavior in certain entities.[11–13] Notably, chromothripsis has been identified to be the major driver of tumor-suppressor gene inactivation and oncogenes amplification, suggesting a pivotal role in both driving and potentially initiating cancer development. One molecular mechanism of chromothripsis-dependent oncogene amplification is through extrachromosomal DNA (ecDNA).[7,11]

The breakthrough in unraveling chromothripsis in cancer is facilitated by the development of computational tools for identifying chromothripsis in cancer using whole-genome sequencing (WGS) data.[11] The landscape of chromothripsis, including its frequency, distribution, intratumoral diversity/heterogeneity, and clinical significance, is not well understood in UC. Moreover, it is unclear how chromothripsis shapes the genomic heterogeneity within cancer cells. To address this, this study provides a comprehensive analysis of the chromothripsis landscape in UC using single-regional and multi-regional WGS data, combined with bulk transcriptome, from a large cohort of UCs (N = 488 patients).

RESULTS

Chromothripsis is a major driver in UC development

To explore the chromothripsis landscape in UC, we performed chromothripsis analysis using ShatterSeek[11] on paired tumor-germline WGS data from our in-house dataset (N = 465 patients) and the Beijing Institute of Genomics (BIG) dataset (N = 3 patients).[14] In addition, we performed multi-regional WGS on 20 UC patients. The entire cohort includes the WGS data from 629 tumors, 491 germline samples, and 166 time-matched urine samples from 488 UC patients (Figure 1A; Tables S1 and S2). Among these patients, 52 (11%) had multi-regional tumor WGS data. The cohort included 362 (74%) males and 126 (26%) females, with a median age of 68 years. Muscle-invasive diseases (pT2-T4) were diagnosed in 232 (48%) patients. Clinical metadata—including age, gender, stage, and survival, as well as sequencing information—are provided in Tables 1 and S1.

The widely accepted model of chromothripsis suggests that, during DNA shattering, some fragments are lost (Figure 1A).[7,11,15] As a result, the oscillation of copy number (CN) between two states serves as a primary indicator of chromothripsis events. We utilized the ShatterSeek[11] method to identify chromothripsis events from paired tumor-germline WGS data (Figure 1A). Based on established criteria,[9,11] chromothripsis events were categorized into high-confidence (HC) and low-confidence (LC) groups. The LC calls involved 4–6 segments between two states, whereas HC calls comprised a minimum of 7 adjacent segments (Figure 1B). Chromothripsis events, including both HC and LC calls, were identified in 41% (199 out of 488) of UC patients (Figure 1C; Table S3), indicating that chromothripsis is a common mutational event in UC. Moreover, about 21% of these events were canonical (Figure 1C), in which more than 60% of CN segments in the affected region exhibited oscillation between the two states. In approximately 86% of tumors, the centromere was included in the segment affected by chromothripsis (Figure S1A). Notably, nearly half (49%, 97 out of 199) of chromothripsis$^+$ UC patients exhibited multiple chromothriptic chromosomes (Figures 1E, S1B, and S1C).

We observed a significant increase in chromothripsis events in patients with muscle-invasive or high-grade tumors compared to those with non-muscle-invasive or low-grade tumors (Figure 1F; grade, p = 3.48e−10; stage, p = 2.11e−07; Fisher's exact test, two-sided). This suggests that chromothripsis occurs during tumor development and might be linked to increased tumor malignancy. Moreover, patients with chromothripsis$^+$ tumors have a poorer prognosis compared to those with chromothripsis$^-$ tumors (Figure 1G; log rank test, p = 3.558e−04). To further assess the prognostic significance of chromothripsis, we performed a Cox proportional hazards regression analysis, adjusting for age, gender, and tumor location. Patients who carried chromothripsis$^+$ tumors exhibited a significantly higher risk of mortality (Figure 1H; hazard ratio = 1.82; $p < 0.001$) compared to patients with chromothripsis$^-$ tumors. These findings highlight chromothripsis as a key driver of UC progression.

Chromothripsis$^+$ tumors have distinct genetic and transcriptional features

Given the significant impact of chromothripsis on UC prognosis, we further investigated the molecular characteristics associated with chromothripsis. Comparative analysis revealed that chromothripsis$^+$ tumors exhibited higher tumor mutation burden (TMB) and structural variants (SVs) compared to chromothripsis$^-$ tumors. Consistently, chromothripsis$^+$ tumors were significantly more chromosomally unstable, as indicated by increased ploidy and a higher fraction of genome altered (FGA) (Figures 2A and S2A; Wilcoxon rank-sum test; TMB, p = 1.5e-05; SV, p = 1.24e−27; ploidy, p = 1.2e−12; FGA, p = 2.3e−16). Genome instability is closely linked to focal amplifications and whole-genome duplication (WGD), both of which were significantly enriched in chromothripsis$^+$ tumors (Figure S2B; Fisher's exact test, two-sided; WGD, p = 1.53e−13; focal amplification, p = 2.72e−21). Additionally, Apolipoprotein B mRNA editing enzyme catalytic polypeptide (APOBEC) mutagenesis, a well-established driver in UC development, was more prevalent in chromothripsis$^+$ tumors, with higher proportions

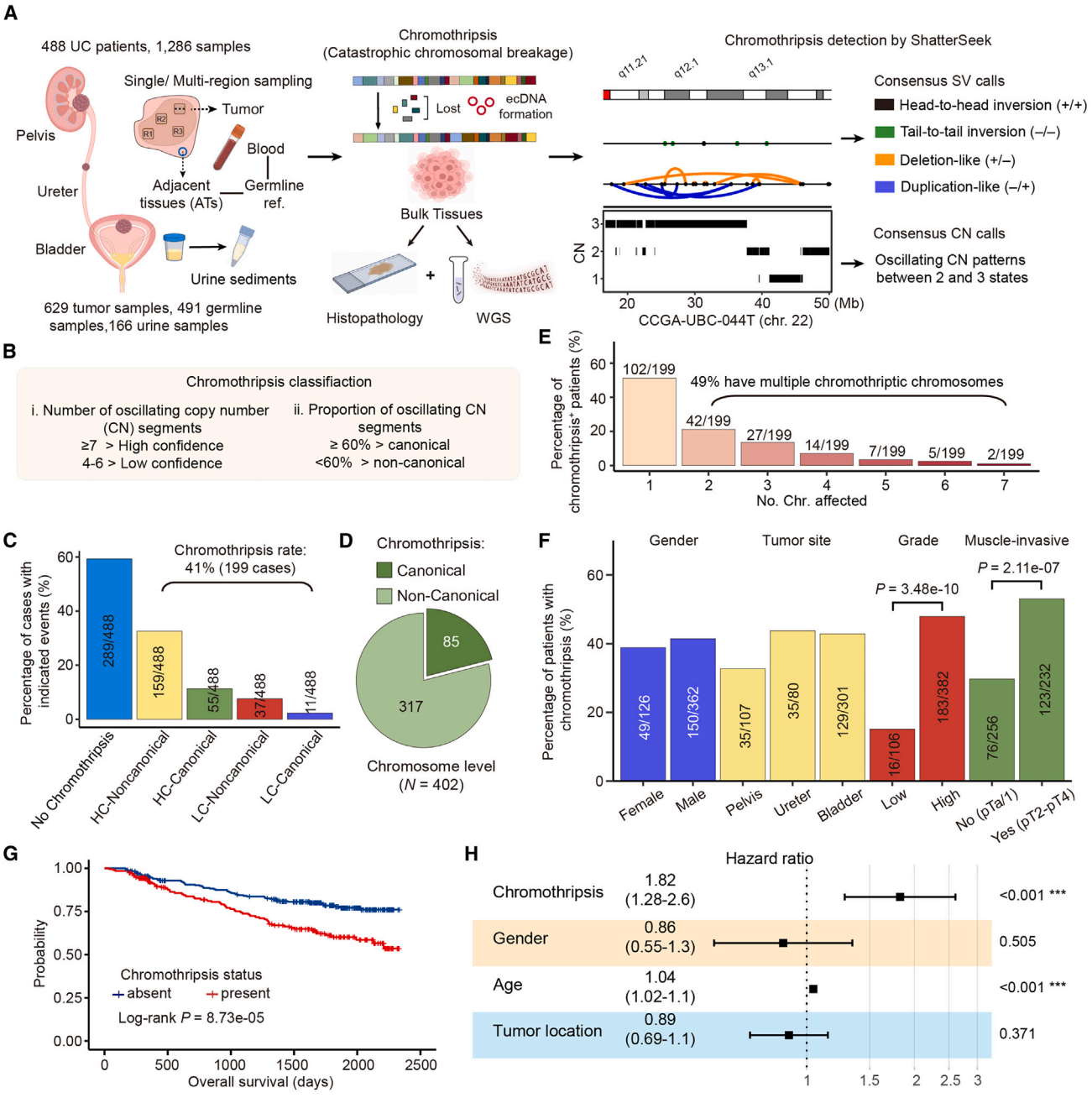

Figure 1. Chromothripsis landscape in UC

(A) Overview of the experimental workflow and a brief model illustrating the process of chromothripsis (created with BioRender.com).

(B) Classification of chromothripsis events into high-confidence (HC) and low-confidence (LC) categories.

(C) Patterns and prevalence of chromothripsis across the entire cohort (488 UC patients).

(D) Percentage of canonical and non-canonical chromothripsis events at the chromosome level (N = 402).

(E) Percentage of patients with single and multiple (2–7) chromothriptic chromosomes.

(F) Presence of chromothripsis by clinical subgroup across 488 UC patients (Fisher's exact test, two-sided).

(G) Kaplan-Meier survival curves illustrating the overall survival of UC patients stratified by chromothripsis status (log rank test).

(H) Hazard ratios with ±95% confidence intervals and p values for chromothripsis status, gender, age, and tumor location calculated using a Cox regression on overall survival.

Table 1. Clinical and WGS information of patients included in the present study

Category	No. (%)
No. of patients	488
Age, yr-no. (%)	
≤65	200 (41)
>65	288 (59)
Gender-no. (%)	
Male	362 (74)
Female	126 (26)
Tumor site-no. (%)	
Pelvis	107 (22)
Ureter	80 (16)
Bladder	301 (62)
Histologic grading-no. (%)	
Low	106 (22)
High	382 (78)
T-category-no. (%)	
Muscle-invasive (pT2-T4)	232 (48)
Non-muscle-invasive (pTa/1)	256 (52)
Multi-regional WGS-no. (%)	
Yes	52 (11)
No	436 (89)

of APOBEC-related signatures observed compared to chromothripsis$^-$ tumors (Figure 2B; Wilcoxon rank-sum test; Catalogue Of Somatic Mutations In Cancer (COSMIC) SBS2, p = 0.0059; COSMIC SBS13, p = 0.0015). Moreover, chromothripsis$^+$ tumors exhibited a significantly higher frequency of alterations in pathways related to the cell cycle (87% vs. 74%; p = 0.0002), TP53 (82% vs. 54%; p = 6.607e−11), WNT signaling pathway (80% vs. 68%; p = 0.005), PI3K signaling pathway (61% vs. 45%; p = 0.0007), MYC signaling pathway (58% vs. 45%; p = 0.006), transforming growth factor β (26% vs. 15%; p = 0.002), and NRF2 (17% vs. 5%; p = 0.0002) pathways[16] (Figure 2C; Fisher's exact test, two-sided). Overall, these data suggested that chromothripsis is linked to an unstable cancer genome in UC.

To further investigate the impact of chromothripsis on transcriptional changes, we compared the transcriptome between chromothripsis$^-$ and chromothripsis$^+$ tumors. Differentially expressed gene (DEG) analysis revealed that 206 genes were specifically up-regulated in chromothripsis$^-$ tumors, while 20 genes showed specific up-regulation in chromothripsis$^+$ tumors (Figure S3A). Enrichment analysis indicated that these genes were predominantly involved in endocytosis, focal adhesion, and mitogen-activated protein kinase signaling pathways (Figure S3B; Table S4). We also examined a curated set of well-defined functional pathways related to UC[5] (Table S5). Notably, chromothripsis$^-$ tumors exhibited remarkably elevated expression of fibroblast growth factor receptor 3 (FGFR3)-associated markers (Figure S3), implying a potential therapeutic benefit from FGFR3 inhibitors. In contrast, chromothripsis$^+$ tumors demonstrated enhanced expression of markers associated with "epithelial-mesenchymal transition (EMT)," "extracellular matrix (ECM)," "smooth muscle," "squamous," and "immune checkpoint" markers (Figure S3). Collectively, these data suggest that chromothripsis is associated with increased genome instability, APOBEC-related mutation burden, and distinct transcriptomic signatures.

TP53 alterations are more frequently detected in chromothripsis$^+$ UC

The tumor suppressor p53, encoded by *TP53*, is crucial for maintaining genome integrity through its roles in DNA damage response, cell-cycle arrest, apoptosis, and inhibition of angiogenesis. Disruption of *TP53* facilitates genomic instability.[17,18] Previous research has shown that *TP53* is frequently subjected to somatic mutations in UC.[2,4,5] To explore the potential relationship between *TP53* alterations and chromothripsis, we analyzed somatic *TP53* mutations in 488 UC cases. We found that *TP53* alterations were significantly more common in chromothripsis$^+$ tumors (52%, 104 out of 199) compared to the chromothripsis$^-$ tumors (25%, 73 out of 289; Fisher exact test, p = 1.31e−09, two-sided) (Figures 2C and S2B), implying a potential mechanism of co-evolution between *TP53* mutation and chromothripsis.

Frequent co-localization of chromothripsis with ecDNA and kataegis

Chromothripsis, followed by circular recombination, contributes to increased gene dosage in cancer.[7,19] To study the relationship between chromothripsis and ecDNA, we applied the AmpliconArchitect[20] method to reconstruct the structure of ecDNA and focal amplification from WGS data. Overall, we identified ecDNA and focal amplification signatures within chromothripsis regions in 9% (18 out of 199) and 29% (57 out of 199) of chromothripsis$^+$ UC patients (Figure S4A; Table S6), suggesting that chromothripsis serves as an initiating event for some ecDNAs or focal amplifications. For example, in CCGA-UBC-075T, we detected *CCND1* (a well-known driver in UC)-containing ecDNA in chromothripsis regions (Figures 3A–3C). *CCND1* amplification was validated by DNA fluorescent *in situ* hybridization (FISH) of interphase spread chromosomes. It is noteworthy that once ecDNA and focal amplification form, the occurrence of chromothripsis phenomena may diminish in the absence of sustained drivers promoting chromosomal instability,[11] which might explain the relatively low co-occurrence frequency of ecDNA (9%)/focal amplification (29%), and chromothripsis may be underestimated. Nevertheless, our results prove that chromothripsis is associated with the genome-wide formation of ecDNA and focal amplification in UC.

Kataegis is a genomic phenomenon characterized by localized clusters of point mutations, often linked to specific mutagenic processes and associated with cancer development. We identified kataegis in 94% of UC patients (458 out of 488). Patients with kataegis mutations exhibited a significantly higher frequency of chromothripsis events compared to those without kataegis (Figure S4B; two-sided Fisher's test, p = 2.933e−06). Furthermore, we examined kataegis occurrences within chromothripsis regions and found that kataegis was present in 57% of these regions (229 out of 402) (Figure S4C). These

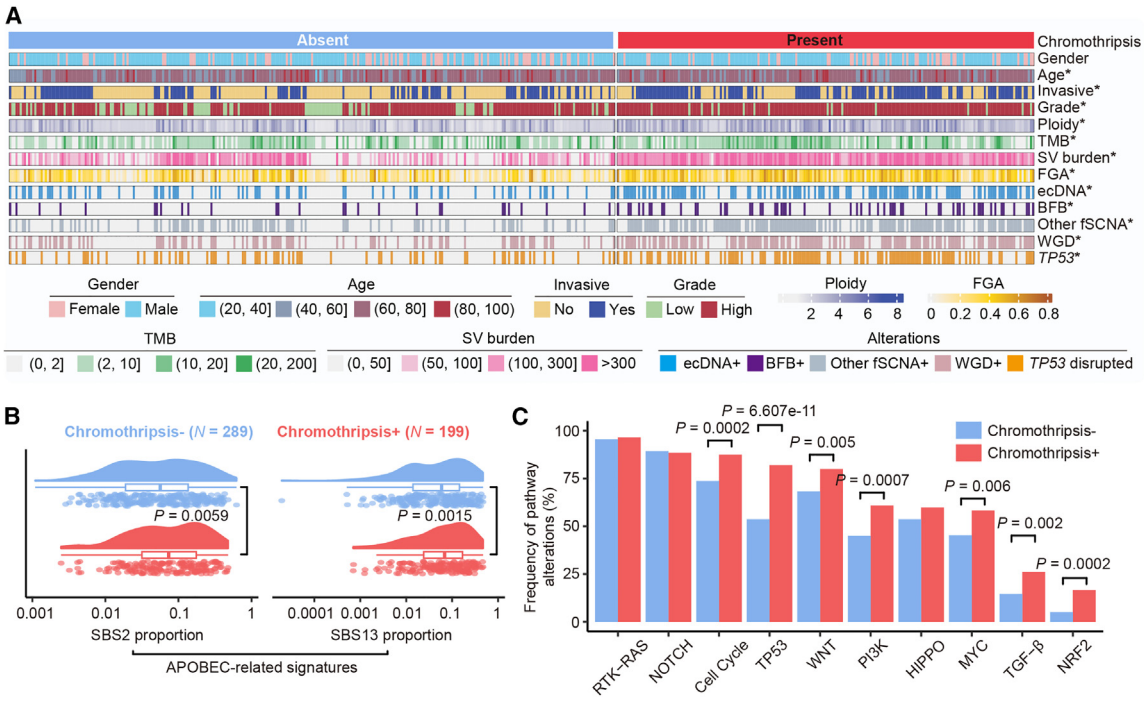

Figure 2. Hallmarks of chromothripsis on UC genome instability, mutation, and transcription

(A) Patient classification by chromothripsis status. The asterisk denotes a statistically significant association with the presence of chromothripsis (Wilcoxon rank-sum test for age, ploidy, TMB, SV burden, and FGA; two-sided Fisher's exact test for other factors). FGA, the fraction of genome altered; TMB, tumor mutation burden; SV, structural variation; fSCNA, focal somatic copy number amplification. BFB, breakage-fusion-bridge; WGD, whole-genome duplication.

(B) Proportion of APOBEC-related mutations (COSMIC SBS2 and SBS13) between chromothripsis^{-} and chromothripsis^{+} tumors (Wilcoxon rank-sum test).

(C) Percentage of patients with alterations for 10 canonical oncogenic pathways (Fisher's exact test, two-sided).

findings corroborate previous observations that chromothripsis frequently co-localizes with kataegis.

The landscape of intratumoral chromothripsis heterogeneity

Chromothripsis represents a significant contributor to intratumor heterogeneity,[21] yet its intertumoral diversity is largely unexplored. We performed multi-regional WGS analysis (two to six tumor regions per patient) from 193 tumors and 52 germline samples, collected across 52 UC patients (Figure 4A). Chromothripsis events were identified in 67% of (35 out of 52) UC cases (Figure 4A). In most chromothripsis^{+} UC patients (86%, 30 out of 35), chromothripsis was selectively detected in specific tumor regions, a phenomenon of intertumoral heterogeneity and referred to as branch chromothripsis hereafter (Figure 4A). In five cases (CUGA-MR-001/023/033/035; CUGA-006), chromothripsis was detected in all analyzed tumor regions (Figures 4A and 4B). For instance, in CUGA-MR-001, we observed chromothripsis events involving chromosomes 6 and 13 were detected only in regions tumor-R3 and lymph node metastasis (LNM) tissues (Figure 4D). The identical chromothripsis event in both primary and metastatic tumor tissue also indicated the involvement of chromothripsis in the process of tumor dissemination. These data suggest that most chromothripsis events are likely a later manifestation of genomic instability and provide a strong selective advantage (Figure 4E).

Discovery of chromothripsis events in the urine of UC patients

We previously demonstrated that extrachromosomal circular DNA with size less than 1 kb (eccDNA) and ecDNA could be detected in urine sediment-derived DNA.[22,23] Therefore, we next sought to investigate if chromothripsis could be detected in the urine, a reservoir of biological waste from the urinary tract. To achieve this, we analyzed WGS data from 166 matched tumor-urine samples. Due to the significantly lower tumor purity in urine sediments (Figure 5B; paired t test, p = 3.79e−23), chromothripsis events were detected in the urinary genomic DNA but less frequently (25%, 42 out of 166) compared to tumor tissues (42%, 70 out of 166) (Figures 5A and 5C). Furthermore, the incidence of chromothripsis in urine was higher in patients with bladder tumors (36%, 33 of 92) than in patients with pelvis (13%, 6 out of 46) or ureter tumors (11%, 3 out of 28) (Figure 5D; Fisher exact test, $p < 0.05$, two-sided). Among 21 patients, chromothripsis was detected in both urine and tumor samples, but the regions of chromothripsis events differed significantly between the two types of samples (Figure S5). Notably, in 13% (21 out of 166) of cases (Figure 5C), chromothripsis was exclusively

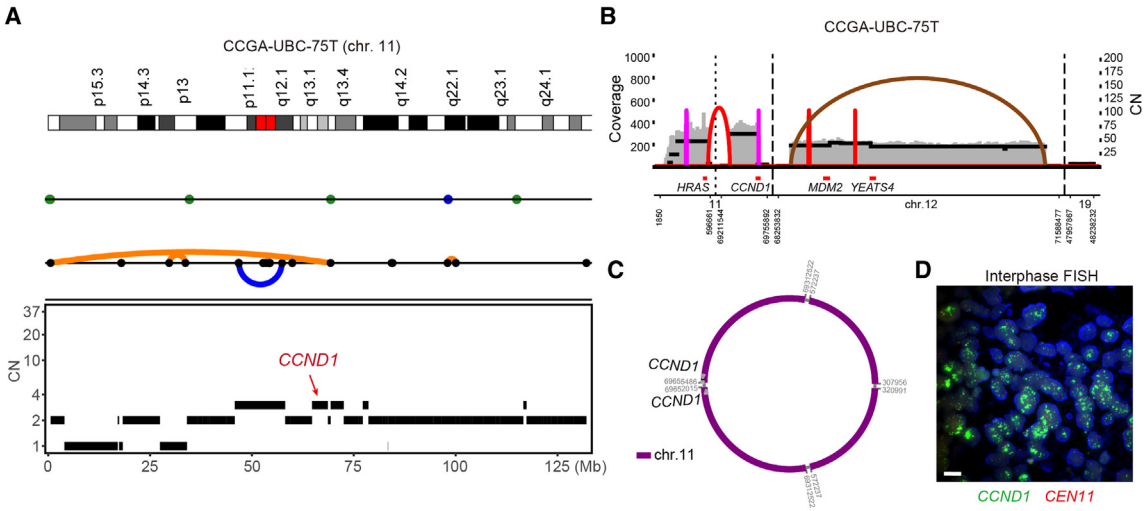

Figure 3. Co-occurrence of chromothripsis with ecDNA and focal amplification

(A) Chromothripsis event (chromosome 11) detected in CCGA-UBC-75T.

(B and C) Structural variant and breakpoint graph (B), along with the structure (C) of the *CCND1*-containing ecDNA identified in CCGA-UBC-75T. The *CCND1*-containing ecDNA is localized within chromothripsis regions.

(D) *CCND1* amplification validated through interphase fluorescent *in situ* hybridization (FISH). Scale bars, 10 μm.

detected in urine samples, further emphasizing the need to consider intratumoral heterogeneity of chromothripsis events in UC.

DISCUSSION

A long-standing challenge in the clinical management of UC is the absence of effective targeted therapeutic drugs, particularly for patients with muscle-invasive disease. Among the limited drugs with Food and Drug Administration-approved usage, FGFR inhibitors such as pemigatinib or erdafitinib currently stand out. By integrating single-regional and multi-regional WGS data from a large cohort of UC patients, we revealed the frequency and diversity of chromothripsis in UC and demonstrated that chromothripsis is a major contributor to UC heterogeneity. Survival analysis revealed that, in comparison to patients with chromothripsis^{-} tumors, those with chromothripsis^{+} tumors are more likely to succumb during the follow-up period. Detecting chromothripsis in UC tumors is crucial in laying the foundation for precision medicine interventions specifically designed to target chromothripsis.

At the genomic level, chromothripsis in UC is associated with extensive CN variations, which are evident in the amplification and deletion patterns observed across multiple chromosomes in our cohort. The presence of multiple chromothriptic chromosomes in nearly half of the chromothripsis^{+} UC patients suggests a recurrent and potentially orchestrated process of genomic disruption. This widespread chromosomal fragmentation likely results from a combination of factors, including DNA replication stress and defective DNA repair mechanisms. To further explore the transcriptional impact of chromothripsis in UC, we found that chromothripsis^{-} tumors had higher expression of FGFR3-related markers, suggesting potential responsiveness to FGFR3 inhibitors. In contrast, chromothripsis^{+} tumors were enriched for markers of EMT, ECM, squamous features, and immune checkpoints, highlighting their distinct transcriptomic profiles and increased genomic instability.

We show the spatial intratumoral heterogeneity of chromothripsis in UC evolution. Even within different tumor regions of the same patient, some tumor regions manifest detectable chromothripsis, while others do not. Previous studies and our data have indicated an association between chromothripsis and drug resistance and tumor metastasis,[19,24] underscoring that targeting trunk driver events (such as *FGFR3* mutations) in cancer treatment may be affected by the occurrence of chromothripsis events in the later stages of tumor evolution. This observation supports ongoing efforts to enhance early detection methods for UC. Moreover, our data emphasize the importance of multi-region tumor sampling for comprehensive chromothripsis profiling.

Considering the clinical implications of chromothripsis, it is crucial to employ non-invasive methods for detecting chromothripsis-driven tumors. Urothelial tumor tissue directly contacts urine, potentially resulting in the presence of tumor cells in the urine. In this study, we decode chromothripsis events from urine samples based on genome sequencing data. We revealed a significantly lower detection rate of chromothripsis in urine (25%) compared to that in tumor tissue (42%). This phenomenon may be explained by the presence of a higher proportion of non-cancerous cells, such as white blood cells, in the urine of UC patients.[25,26] Further studies could explore the potential of initially enriching tumor cells from the urine of cancer patients, followed by chromothripsis detection. Identifying chromothripsis in urine samples opens a wide range of diagnostic opportunities in genitourinary tumors.

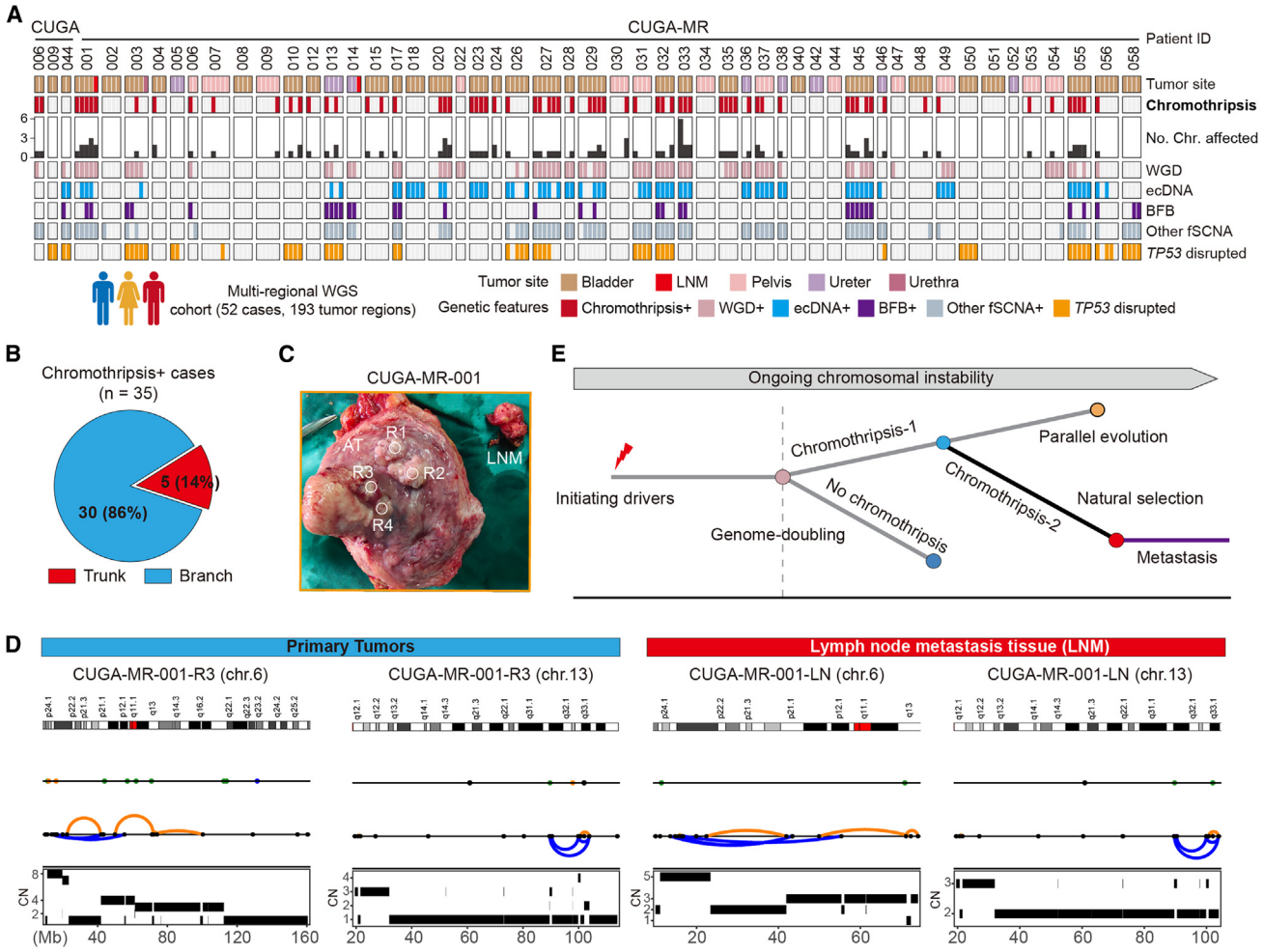

Figure 4. Intratumoral chromothripsis heterogeneity in UC

(A) Oncoprint tables of samples from the multi-regional WGS cohort (*N* = 193 tumors from 52 patients are shown). Each column represents one tumor. Genetic alterations, including chromothripsis, WGD, ecDNA, BFB, other fSCNA, and *TP53* disrupted, as well as the number of chromosomes affected by chromothripsis, are indicated. fSCNA, focal somatic copy number amplification. BFB, breakage-fusion-bridge; WGD, whole-genome duplication.

(B) Proportion of trunk and branch chromothripsis events across 35 patients with chromothripsis^{+} tumors. A trunk chromothripsis event was defined as chromothripsis detectable across all tumor regions in the same patient, while a branch chromothripsis event was specific to specific tumor regions.

(C) Representative images illustrating the multi-regional sampling sites of patient CUGA-MR-001.

(D) Example of heterogeneous chromothripsis events involving chromosomes 6 and 13, detected in regions R3 and LNM from patient CUGA-MR-001.

(E) A schematic illustration of chromothripsis evolution in cancer. Initiating driver instigates the initiation of tumors. After genome doubling of cancer cells, a subset of cancer cells experiences chromothripsis events, while others do not. As the tumor progresses, cells with chromothripsis undergo parallel evolution, whereas another subset, under the pressure of natural selection, generates new chromothripsis events and actively contributes to tumor metastasis. These dynamic processes collectively contribute to the subclonal evolution of the tumor.

Chromothripsis has been implicated in intratumoral heterogeneity. In this study, we have shown that chromothripsis is an independent prognostic factor for UC patients. It is associated with increased mutational load, higher genome instability, oncogene amplification, and tumor dissemination. Further studies of the mechanisms of chromothripsis formation and maintenance may uncover new combinatorial therapies for UC patients.

Limitations of the study

The study primarily focused on the frequency and characteristics of chromothripsis but did not investigate the underlying mechanisms or potential therapeutic implications. Future studies should address these limitations and explore the broader implications of chromothripsis in cancer development and treatment.

RESOURCE AVAILABILITY

Lead contact

Requests for further information and resources should be directed to and will be fulfilled by the lead contact, Yonglun Luo (alun@biomed.au.dk).

Materials availability

This study did not generate new unique reagents.

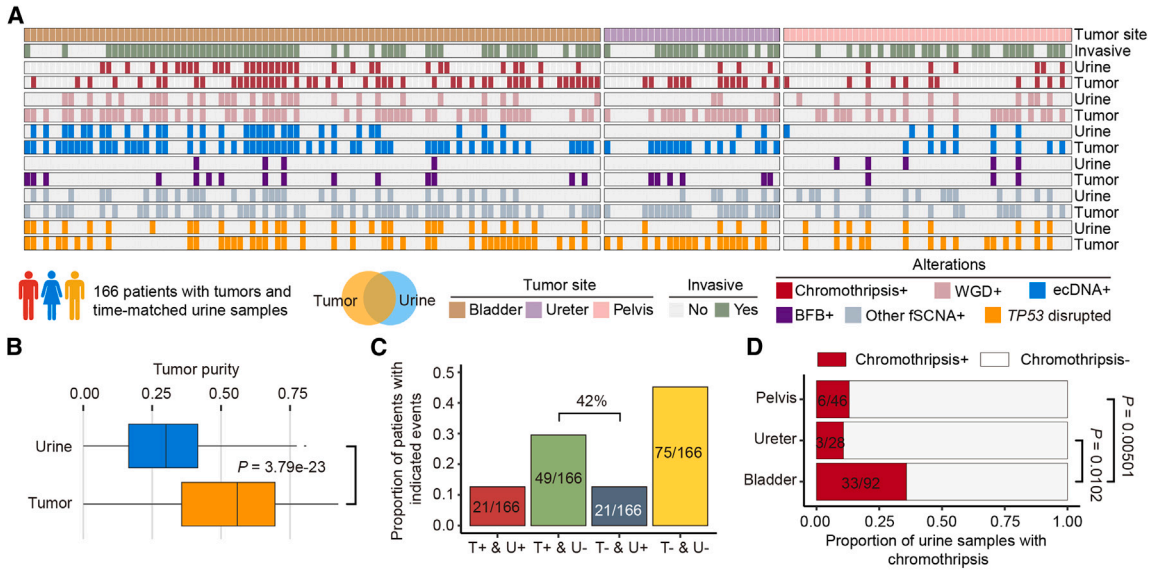

Figure 5. Discovery of chromothripsis in urinary genomic DNA from UC

(A) Chromothripsis and other genetic alterations in paired tumor and urine samples (N = 166). Each column represents one patient. Each row indicates genetic alterations detected in preoperative urine sediment (indicated by ''U") and paired tumors (indicated by ''T").

(B) Comparison of the tumor purity between urine and paired tumor samples (paired t test). Tumor purity was calculated from WGS data using the FACETS algorithm. Values are represented as median with 25th and 75th percentile.

(C) Proportion of patients with indicated events: T^+ & U^+: chromothripsis detected in both tumor and urine samples. T^+ & U^-: chromothripsis detected only in tumors. T^- & U^+: chromothripsis detected only in urine. T^- & U^-: chromothripsis undetected in both tumor and urine samples.

(D) Proportion of urine samples with chromothripsis, stratified by tumor location (Fisher's exact test, two-sided).

Data and code availability

- WGS and RNA sequencing data have been deposited at Genome Sequence Archive (GSA) as HRA005963, HRA003461, HRA004718, and HRA005001 and China National GeneBank as CNP0003498 and are publicly available as of the date of publication.
- This paper does not report original code.
- Any additional information required to reanalyze the data reported in this paper is available from the lead contact upon request.

ACKNOWLEDGMENTS

We gratefully acknowledge the contributions of our patients who participated in the study and their families. This work was jointly supported by IBMC-BGI Center, Qingdao-Europe Advanced Institute for Life Sciences, Taishan Scholar Program (no. Tsqn202103198), the Shandong Provincial Medical Association Clinical Research Funds Qilu Special (YXH2022ZX02181), the Jinan Science and Technology Plan-Clinical Medical Science and Technology Innovation Program (no. 202134003 and no. 202225057), and the First Affiliated Hospital of Shandong First Medical University National Natural Science Foundation Cultivation Program (QYPY2020NSFC0616). W.L. was supported by the China Scholarship Council (CSC). We thank the support from China National GeneBank. Y. Luo is supported by the Danish Research Council (9041-00317B), European Union's Horizon 2020 research and innovation program under grant agreement no. 899417, the Novo Nordisk Foundation (NNF21OC0068988; NNF21OC0071031), M-ERA.Net and the Innovation Fund Denmark (9355 PIECRISCI), and the Lundbeck Foundation Ascending Investigator award (R396-2022-350).

AUTHOR CONTRIBUTIONS

W.L., P.H., Y. Luo, and C. Lin contributed to the study design and conceptualization. P.H., Y. Luo, C. Lin, W.L., X.J., and X.S. co-supervised the project. P.H., C. Lin, Y. Luo, and X.S. acquired funding. C. Lin, Y.L., T.Y., S.W., N.L., W.W., J.M., and X.C. contributed to the sample and information collection. Y.L. provided WGS and clinical data for the BIG cohort. P.H. and W.L. performed WGS production. W.D., H.Y., and M.Z. provided computational resources. W.L., Y.Z., H. Tao, C.L., and S.J. contributed to computational data analysis. Y.L., H. Tao, X.C., T.F., K.C., K.M., and P.W. assisted with data analysis. Y.Z., H.T., C.C., and Z.X. uploaded the raw sequencing data to GSA. Y. Luo., B.L., L.L., and W.L. supervised the data analysis, data integration, and interpretation. W.L., Y.Z., C.L., and H. Tao. prepared and modified the figures. W.L. wrote the manuscript with input from Y.Z., H.T., and C.L. Y. Luo, P.H., and W.L. revised the manuscript. All authors discussed the results and contributed to the review and editing of the manuscript.

DECLARATION OF INTERESTS

The authors declare no competing interests.

STAR★METHODS

Detailed methods are provided in the online version of this paper and include the following:

- KEY RESOURCES TABLE
- EXPERIMENTAL MODEL AND STUDY PARTICIPANT DETAILS
  - Human samples
- METHOD DETAILS
  - Datasets
  - Genomic DNA isolation
  - Whole genome sequencing (WGS)
  - WGS processing
  - Variant calling
  - Kataegis detection
  - Chromothripsis calling
  - Focal amplifications calling

- Mutational signature analysis
- CNV signature quantification
- Processing of RNA-seq data
- Interphase FISH
- Analysis of clinical outcomes

- QUANTIFICATION AND STATISTICAL ANALYSIS

SUPPLEMENTAL INFORMATION

Supplemental information can be found online at https://doi.org/10.1016/j.isci.2024.111510.

Received: January 30, 2024
Revised: August 24, 2024
Accepted: November 28, 2024
Published: December 2, 2024

REFERENCES

1. Flaig, T.W., Spiess, P.E., Abern, M., Agarwal, N., Bangs, R., Buyyounouski, M.K., Chan, K., Chang, S.S., Chang, P., Friedlander, T., et al. (2024). NCCN Guidelines® Insights: Bladder Cancer, Version 3.2024. J. Natl. Compr. Cancer Netw. *22*, 216–225. https://doi.org/10.6004/jnccn.2024.0024.
2. Tran, L., Xiao, J.F., Agarwal, N., Duex, J.E., and Theodorescu, D. (2021). Advances in bladder cancer biology and therapy. Nat. Rev. Cancer *21*, 104–121. https://doi.org/10.1038/s41568-020-00313-1.
3. Glaser, A.P., Fantini, D., Shilatifard, A., Schaeffer, E.M., and Meeks, J.J. (2017). The evolving genomic landscape of urothelial carcinoma. Nat. Rev. Urol. *14*, 215–229. https://doi.org/10.1038/nrurol.2017.11.
4. Sfakianos, J.P., Cha, E.K., Iyer, G., Scott, S.N., Zabor, E.C., Shah, R.H., Ren, Q., Bagrodia, A., Kim, P.H., Hakimi, A.A., et al. (2015). Genomic Characterization of Upper Tract Urothelial Carcinoma. Eur. Urol. *68*, 970–977. https://doi.org/10.1016/j.eururo.2015.07.039.
5. Fujii, Y., Sato, Y., Suzuki, H., Kakiuchi, N., Yoshizato, T., Lenis, A.T., Maekawa, S., Yokoyama, A., Takeuchi, Y., Inoue, Y., et al. (2021). Molecular classification and diagnostics of upper urinary tract urothelial carcinoma. Cancer Cell *39*, 793–809.e8. https://doi.org/10.1016/j.ccell.2021.05.008.
6. Robertson, A.G., Kim, J., Al-Ahmadie, H., Bellmunt, J., Guo, G., Cherniack, A.D., Hinoue, T., Laird, P.W., Hoadley, K.A., Akbani, R., et al. (2017). Comprehensive Molecular Characterization of Muscle-Invasive Bladder Cancer. Cell *171*, 540–556.e25. https://doi.org/10.1016/j.cell.2017.09.007.
7. Stephens, P.J., Greenman, C.D., Fu, B., Yang, F., Bignell, G.R., Mudie, L.J., Pleasance, E.D., Lau, K.W., Beare, D., Stebbings, L.A., et al. (2011). Massive genomic rearrangement acquired in a single catastrophic event during cancer development. Cell *144*, 27–40. https://doi.org/10.1016/j.cell.2010.11.055.
8. Zhang, C.Z., Spektor, A., Cornils, H., Francis, J.M., Jackson, E.K., Liu, S., Meyerson, M., and Pellman, D. (2015). Chromothripsis from DNA damage in micronuclei. Nature *522*, 179–184. https://doi.org/10.1038/nature14493.
9. Korbel, J.O., and Campbell, P.J. (2013). Criteria for inference of chromothripsis in cancer genomes. Cell *152*, 1226–1236. https://doi.org/10.1016/j.cell.2013.02.023.
10. Leibowitz, M.L., Zhang, C.Z., and Pellman, D. (2015). Chromothripsis: A New Mechanism for Rapid Karyotype Evolution. Annu. Rev. Genet. *49*, 183–211. https://doi.org/10.1146/annurev-genet-120213-092228.
11. Cortés-Ciriano, I., Lee, J.J.K., Xi, R., Jain, D., Jung, Y.L., Yang, L., Gordenin, D., Klimczak, L.J., Zhang, C.Z., Pellman, D.S., et al. (2020). Comprehensive analysis of chromothripsis in 2,658 human cancers using whole-genome sequencing. Nat. Genet. *52*, 331–341. https://doi.org/10.1038/s41588-019-0576-7.
12. Voronina, N., Wong, J.K.L., Hübschmann, D., Hlevnjak, M., Uhrig, S., Heilig, C.E., Horak, P., Kreutzfeldt, S., Mock, A., Stenzinger, A., et al. (2020). The landscape of chromothripsis across adult cancer types. Nat. Commun. *11*, 2320. https://doi.org/10.1038/s41467-020-16134-7.
13. Bolkestein, M., Wong, J.K.L., Thewes, V., Körber, V., Hlevnjak, M., Elgaafary, S., Schulze, M., Kommoss, F.K.F., Sinn, H.P., Anzeneder, T., et al. (2020). Chromothripsis in Human Breast Cancer. Cancer Res. *80*, 4918–4931. https://doi.org/10.1158/0008-5472.Can-20-1920.
14. Lu, H., Liang, Y., Guan, B., Shi, Y., Gong, Y., Li, J., Kong, W., Liu, J., Fang, D., Liu, L., et al. (2020). Aristolochic acid mutational signature defines the low-risk subtype in upper tract urothelial carcinoma. Theranostics *10*, 4323–4333. https://doi.org/10.7150/thno.43251.
15. Li, Y., Schwab, C., Ryan, S., Papaemmanuil, E., Robinson, H.M., Jacobs, P., Moorman, A.V., Dyer, S., Borrow, J., Griffiths, M., et al. (2014). Constitutional and somatic rearrangement of chromosome 21 in acute lymphoblastic leukaemia. Nature *508*, 98–102. https://doi.org/10.1038/nature13115.
16. Sanchez-Vega, F., Mina, M., Armenia, J., Chatila, W.K., Luna, A., La, K.C., Dimitriadoy, S., Liu, D.L., Kantheti, H.S., Saghafinia, S., et al. (2018). Oncogenic Signaling Pathways in The Cancer Genome Atlas. Cell *173*, 321–337.e10. https://doi.org/10.1016/j.cell.2018.03.035.
17. Hanel, W., and Moll, U.M. (2012). Links between mutant p53 and genomic instability. J. Cell. Biochem. *113*, 433–439. https://doi.org/10.1002/jcb.23400.
18. Eischen, C.M. (2016). Genome Stability Requires p53. Cold Spring Harbor Perspect. Med. *6*, a026096. https://doi.org/10.1101/cshperspect.a026096.
19. Shoshani, O., Brunner, S.F., Yaeger, R., Ly, P., Nechemia-Arbely, Y., Kim, D.H., Fang, R., Castillon, G.A., Yu, M., Li, J.S.Z., et al. (2021). Chromothripsis drives the evolution of gene amplification in cancer. Nature *591*, 137–141. https://doi.org/10.1038/s41586-020-03064-z.
20. Deshpande, V., Luebeck, J., Nguyen, N.P.D., Bakhtiari, M., Turner, K.M., Schwab, R., Carter, H., Mischel, P.S., and Bafna, V. (2019). Exploring the landscape of focal amplifications in cancer using AmpliconArchitect. Nat. Commun. *10*, 392. https://doi.org/10.1038/s41467-018-08200-y.
21. Vitale, I., Shema, E., Loi, S., and Galluzzi, L. (2021). Intratumoral heterogeneity in cancer progression and response to immunotherapy. Nat. Med. *27*, 212–224. https://doi.org/10.1038/s41591-021-01233-9.
22. Lv, W., Pan, X., Han, P., Wang, Z., Feng, W., Xing, X., Wang, Q., Qu, K., Zeng, Y., Zhang, C., et al. (2022). Circle-Seq reveals genomic and disease-specific hallmarks in urinary cell-free extrachromosomal circular DNAs. Clin. Transl. Med. *12*, e817. https://doi.org/10.1002/ctm2.817.
23. Lv, W., Pan, X., Han, P., Wu, S., Zeng, Y., Wang, Q., Guo, L., Xu, M., Qi, Y., Deng, L., et al. (2024). Extrachromosomal circular DNA orchestrates genome heterogeneity in urothelial bladder carcinoma. Theranostics *14*, 5102–5122. https://doi.org/10.7150/thno.99563.
24. Rode, A., Maass, K.K., Willmund, K.V., Lichter, P., and Ernst, A. (2016). Chromothripsis in cancer cells: An update. Int. J. Cancer *138*, 2322–2333. https://doi.org/10.1002/ijc.29888.
25. Rose, K.M., Huelster, H.L., Meeks, J.J., Faltas, B.M., Sonpavde, G.P., Lerner, S.P., Ross, J.S., Spiess, P.E., Grass, G.D., Jain, R.K., et al. (2023). Circulating and urinary tumour DNA in urothelial carcinoma - upper tract, lower tract and metastatic disease. Nat. Rev. Urol. *20*, 406–419. https://doi.org/10.1038/s41585-023-00725-2.
26. Zeng, Y., Wang, A., Lv, W., Wang, Q., Jiang, S., Pan, X., Wang, F., Yang, H., Bolund, L., Lin, C., et al. (2023). Recent development of urinary biomarkers for bladder cancer diagnosis and monitoring. Clin. Transl. Discov. *3*, e183. https://doi.org/10.1002/ctd2.183.
27. Chen, S., Zhou, Y., Chen, Y., and Gu, J. (2018). fastp: an ultra-fast all-in-one FASTQ preprocessor. Bioinformatics *34*, i884–i890. https://doi.org/10.1093/bioinformatics/bty560.
28. Vasimuddin, M., Misra, S., Li, H., and Aluru, S. (2019). Efficient Architecture-Aware Acceleration of BWA-MEM for Multicore Systems. In

2019 IEEE international parallel and distributed processing symposium (IPDPS) (IEEE), pp. 314–324.

29. Li, H., Handsaker, B., Wysoker, A., Fennell, T., Ruan, J., Homer, N., Marth, G., Abecasis, G., and Durbin, R.; 1000 Genome Project Data Processing Subgroup (2009). The Sequence Alignment/Map format and SAMtools. Bioinformatics *25*, 2078–2079. https://doi.org/10.1093/bioinformatics/btp352.
30. Cibulskis, K., Lawrence, M.S., Carter, S.L., Sivachenko, A., Jaffe, D., Sougnez, C., Gabriel, S., Meyerson, M., Lander, E.S., and Getz, G. (2013). Sensitive detection of somatic point mutations in impure and heterogeneous cancer samples. Nat. Biotechnol. *31*, 213–219. https://doi.org/10.1038/nbt.2514.
31. Kim, S., Scheffler, K., Halpern, A.L., Bekritsky, M.A., Noh, E., Källberg, M., Chen, X., Kim, Y., Beyter, D., Krusche, P., and Saunders, C.T. (2018). Strelka2: fast and accurate calling of germline and somatic variants. Nat. Methods *15*, 591–594. https://doi.org/10.1038/s41592-018-0051-x.
32. Wang, K., Li, M., and Hakonarson, H. (2010). ANNOVAR: functional annotation of genetic variants from high-throughput sequencing data. Nucleic Acids Res. *38*, e164. https://doi.org/10.1093/nar/gkq603.
33. Lek, M., Karczewski, K.J., Minikel, E.V., Samocha, K.E., Banks, E., Fennell, T., O'Donnell-Luria, A.H., Ware, J.S., Hill, A.J., Cummings, B.B., et al. (2016). Analysis of protein-coding genetic variation in 60,706 humans. Nature *536*, 285–291. https://doi.org/10.1038/nature19057.
34. Landrum, M.J., Lee, J.M., Benson, M., Brown, G.R., Chao, C., Chitipiralla, S., Gu, B., Hart, J., Hoffman, D., Jang, W., et al. (2018). ClinVar: improving access to variant interpretations and supporting evidence. Nucleic Acids Res. *46*, D1062–D1067. https://doi.org/10.1093/nar/gkx1153.
35. Rausch, T., Zichner, T., Schlattl, A., Stütz, A.M., Benes, V., and Korbel, J.O. (2012). DELLY: structural variant discovery by integrated paired-end and split-read analysis. Bioinformatics *28*, i333–i339. https://doi.org/10.1093/bioinformatics/bts378.
36. Wala, J.A., Bandopadhayay, P., Greenwald, N.F., O'Rourke, R., Sharpe, T., Stewart, C., Schumacher, S., Li, Y., Weischenfeldt, J., Yao, X., et al. (2018). SvABA: genome-wide detection of structural variants and indels by local assembly. Genome Res. *28*, 581–591. https://doi.org/10.1101/gr.221028.117.
37. Layer, R.M., Chiang, C., Quinlan, A.R., and Hall, I.M. (2014). LUMPY: a probabilistic framework for structural variant discovery. Genome Biol. *15*, R84. https://doi.org/10.1186/gb-2014-15-6-r84.
38. Chen, X., Schulz-Trieglaff, O., Shaw, R., Barnes, B., Schlesinger, F., Källberg, M., Cox, A.J., Kruglyak, S., and Saunders, C.T. (2016). Manta: rapid detection of structural variants and indels for germline and cancer sequencing applications. Bioinformatics *32*, 1220–1222. https://doi.org/10.1093/bioinformatics/btv710.
39. Jeffares, D.C., Jolly, C., Hoti, M., Speed, D., Shaw, L., Rallis, C., Balloux, F., Dessimoz, C., Bähler, J., and Sedlazeck, F.J. (2017). Transient structural variations have strong effects on quantitative traits and reproductive isolation in fission yeast. Nat. Commun. *8*, 14061. https://doi.org/10.1038/ncomms14061.
40. Shen, R., and Seshan, V.E. (2016). FACETS: allele-specific copy number and clonal heterogeneity analysis tool for high-throughput DNA sequencing. Nucleic Acids Res. *44*, e131. https://doi.org/10.1093/nar/gkw520.
41. Bielski, C.M., Zehir, A., Penson, A.V., Donoghue, M.T.A., Chatila, W., Armenia, J., Chang, M.T., Schram, A.M., Jonsson, P., Bandlamudi, C., et al. (2018). Genome doubling shapes the evolution and prognosis of advanced cancers. Nat. Genet. *50*, 1189–1195. https://doi.org/10.1038/s41588-018-0165-1.
42. Talevich, E., Shain, A.H., Botton, T., and Bastian, B.C. (2016). CNVkit: Genome-Wide Copy Number Detection and Visualization from Targeted DNA Sequencing. PLoS Comput. Biol. *12*, e1004873. https://doi.org/10.1371/journal.pcbi.1004873.
43. Mermel, C.H., Schumacher, S.E., Hill, B., Meyerson, M.L., Beroukhim, R., and Getz, G. (2011). GISTIC2.0 facilitates sensitive and confident localization of the targets of focal somatic copy-number alteration in human cancers. Genome Biol. *12*, R41. https://doi.org/10.1186/gb-2011-12-4-r41.
44. Mayakonda, A., Lin, D.C., Assenov, Y., Plass, C., and Koeffler, H.P. (2018). Maftools: efficient and comprehensive analysis of somatic variants in cancer. Genome Res. *28*, 1747–1756. https://doi.org/10.1101/gr.239244.118.
45. Luebeck, J., Ng, A.W.T., Galipeau, P.C., Li, X., Sanchez, C.A., Katz-Summercorn, A.C., Kim, H., Jammula, S., He, Y., Lippman, S.M., et al. (2023). Extrachromosomal DNA in the cancerous transformation of Barrett's oesophagus. Nature *616*, 798–805. https://doi.org/10.1038/s41586-023-05937-5.
46. Kim, H., Nguyen, N.P., Turner, K., Wu, S., Gujar, A.D., Luebeck, J., Liu, J., Deshpande, V., Rajkumar, U., Namburi, S., et al. (2020). Extrachromosomal DNA is associated with oncogene amplification and poor outcome across multiple cancers. Nat. Genet. *52*, 891–897. https://doi.org/10.1038/s41588-020-0678-2.
47. Blokzijl, F., Janssen, R., van Boxtel, R., and Cuppen, E. (2018). MutationalPatterns: comprehensive genome-wide analysis of mutational processes. Genome Med. *10*, 33. https://doi.org/10.1186/s13073-018-0539-0.
48. Dobin, A., Davis, C.A., Schlesinger, F., Drenkow, J., Zaleski, C., Jha, S., Batut, P., Chaisson, M., and Gingeras, T.R. (2013). STAR: ultrafast universal RNA-seq aligner. Bioinformatics *29*, 15–21. https://doi.org/10.1093/bioinformatics/bts635.
49. Li, B., and Dewey, C.N. (2011). RSEM: accurate transcript quantification from RNA-Seq data with or without a reference genome. BMC Bioinf. *12*, 323. https://doi.org/10.1186/1471-2105-12-323.
50. Hänzelmann, S., Castelo, R., and Guinney, J. (2013). GSVA: gene set variation analysis for microarray and RNA-seq data. BMC Bioinf. *14*, e183. https://doi.org/10.1186/1471-2105-14-7.
51. Love, M.I., Huber, W., and Anders, S. (2014). Moderated estimation of fold change and dispersion for RNA-seq data with DESeq2. Genome Biol. *15*, 550. https://doi.org/10.1186/s13059-014-0550-8.
52. Wu, T., Hu, E., Xu, S., Chen, M., Guo, P., Dai, Z., Feng, T., Zhou, L., Tang, W., Zhan, L., et al. (2021). clusterProfiler 4.0: A universal enrichment tool for interpreting omics data. Innovation *2*, 100141. https://doi.org/10.1016/j.xinn.2021.100141.

STAR★METHODS

KEY RESOURCES TABLE

REAGENT or RESOURCE	SOURCE	IDENTIFIER
Biological samples		
71 tumors and 20 adjacent tumor samples from 20 UC patients	This paper	
Critical commercial assays		
MagAttract HMW DNA kit	Qiagen	67563
Qubit dsDNA HS Assay kit	Invitrogen	Q32851
MGIEasy DNA Library Preparation Kit	MGI	1000006985
ZytoLight® SPEC CCND1/CEN11 Dual Color Probe	ZytoVision	Z-2071-200
Deposited data		
In-house-This study Data	This paper, GSA-Human: HRA005963	https://ngdc.cncb.ac.cn/gsa-human/s/CGL69Tjc
Raw sequencing data of three paired tumor-germline WGS-data from the BIG dataset	GSA-Human: HRA000029; GVM: GVM000054	https://ngdc.cncb.ac.cn/gsa-human/browse/HRA000029; https://ngdc.cncb.ac.cn/gvm/getProjectDetail?project=GVM000054
In-house Data	GSA-Human: HRA003461, HRA004718, HRA005001; CNGB: CNP0003498	https://ngdc.cncb.ac.cn/gsa-human/browse/HRA003461, https://ngdc.cncb.ac.cn/gsa-human/s/Mbxq9RV8, https://ngdc.cncb.ac.cn/gsa-human/s/qTvrKj89, https://db.cngb.org/search/project/CNP0003498/
Software and algorithms		
R (v4.2.2)	R Foundation	https://www.r-project.org/
ShatterSeek (version1.1)	Cortés-Ciriano et al.[11]	https://github.com/parklab/shatterseek/
bwa (version 0.7.17)	Li et al.[27]	http://bio-bwa.sourceforge.net/bwa.shtml
samtools (version 1.11)	Li et al.[28]	http://samtools.sourceforge.net/
fastQC (version 0.11.7)	Babraham Bioinformatics	https://www.bioinformatics.babraham.ac.uk/projects/fastqc/
fastp (version 0.23.2)	Chen et al.[29]	https://github.com/OpenGene/fastp
Perl (version 5.16.3)	Larry Arnold Wall	http://www.perl.org
Java (version 1.8.0_262)	/	https://www.oracle.com/java
Mutect2 (version 4.2.5.0)	Cibulskis et al.[30]	https://gatk.broadinstitute.org/
ANNOVAR (version 2020.06.07)	Wang et al.[31]	http://www.openbioinformatics.org/annovar/
AmpliconSuite-pipeline (version 1.0.0)	Deshpande et al.[20]	https://github.com/AmpliconSuite/AmpliconSuite-pipeline
AmpliconArchitect (version 1.3.r6)	Deshpande et al.[20]	https://github.com/AmpliconSuite/AmpliconArchitect
AmpliconClassifier (version 1.0.0)	Deshpande et al.[20]	https://github.com/jluebeck/AmpliconClassifier
CycleViz (version 0.1.5)	Deshpande et al.[20]	https://github.com/jluebeck/CycleViz
MutationalPatterns (version 3.8.1)	Blokzijl et al.[32]	https://bioconductor.org/packages/release/bioc/html/MutationalPatterns.html
Bedtools (version 2.30.0)	Quinlan laboratory	https://bedtools.readthedocs.io/en/latest/
gistic2 (version 2.0.23)	Mermel et al.[33]	https://broadinstitute.github.io/gistic2/
CNVkit (version 0.9.9)	Talevich et al.[34]	https://cnvkit.readthedocs.io/en/stable/
Delly2 (version 1.1.3)	Rausch et al.[35]	https://tobiasrausch.com/delly/
Manta (version 1.6.0)	Chen et al.[36]	https://github.com/Illumina/manta
SvABA (version 1.1.0)	Wala et al.[37]	https://github.com/walaj/svaba
Lumpy (version 0.2.13)	Layer et al.[38]	https://github.com/arq5x/lumpy-sv
SURVIVOR (version 1.0.7)	Jeffares et al.[39]	https://github.com/fritzsedlazeck/SURVIVOR

(*Continued on next page*)

Continued

REAGENT or RESOURCE	SOURCE	IDENTIFIER
FACETS (version 0.5.14)	Shen et al.[40]	https://github.com/mskcc/facets
TrimGalore (version 0.6.7)	/	https://github.com/FelixKrueger/TrimGalore
STAR (version 2.7.10a)	Dobin et al.[41]	https://github.com/alexdobin/STAR
RSEM (version 1.3.3)	Li et al.[42]	https://github.com/deweylab/RSEM
DESeq2 (version 1.40.2)	Love et al.[43]	https://github.com/thelovelab/DESeq2
ClusterProfiler (version 4.6.2)	Wu et al.[44]	https://github.com/YuLab-SMU/clusterProfiler
GSVA (version 1.46.0)	Hänzelmann et al.[45]	https://github.com/rcastelo/GSVA
maftools (version 2.14.0)	Mayakonda et al.[46]	https://github.com/PoisonAlien/maftools
survminer (version 0.4.9)	Alboukadel Kassambara et al.	https://rpkgs.datanovia.com/survminer/index.html

EXPERIMENTAL MODEL AND STUDY PARTICIPANT DETAILS

Human samples

We collected 71 tumors and 20 adjacent tumor samples from 20 UC patients, who had not undergone systemic therapy before surgery. There was no selection of patients for specific clinical features. For multifocal urothelial tumors, we sampled tissues from different sites, while for solitary urothelial tumors, we collected samples from distinct tumor regions that were at least 5 mm apart and located away from the tumor margin. Paired adjacent tumor tissues (ATs) were collected at a minimum distance of 2 cm from the tumor margin. To ensure privacy, the identifiers of patients were reassigned. Tissue samples were promptly collected within 30 minutes post-surgery and immediately snap-frozen in liquid nitrogen for subsequent processing. The histology of tumors was evaluated by three pathologists. The study adhered to both national and local laws and regulations and received approval from the Research Ethics Committee of Yantai Yuhuangding Hospital. Before enrollment, all participating patients provided written informed consent, and no compensation was provided for their participation.

METHOD DETAILS

Datasets

We collected WGS data from 558 tumors, 471 germline samples, and 166 urine samples, along with RNA-seq data from 328 tumors sourced from both our in-house and BIG datasets.[14] Clinical and sequencing information of included patients is provided in Tables S1 and S2.

Genomic DNA isolation

Genomic DNA was isolated from fresh frozen tissues using the MagAttract HMW DNA kit (Qiagen) according to the manufacturer's instructions. The concentration and integrity of DNA were assessed using Qubit dsDNA BR (Invitrogen) and electrophoresis on a 0.8% agarose gel, respectively.

Whole genome sequencing (WGS)

500 ng of genomic DNA was subjected to the WGS library construction using the MGIEasy DNA Library Preparation Kit (MGI). Briefly, the genomic DNA was fragmented, ligated with adapters, and subjected to PCR amplification. The constructed libraries were quality-controlled using the Qubit dsDNA HS (Invitrogen), and Agilent 2100 system, and were deep sequenced on DNBSEQ with 150 bp paired-end reads.

WGS processing

FastQC (v0.11.7) was performed to assess the sequencing quality of FASTQ files. Subsequently, fastp[27] (v0.23.2) was utilized to trim reads of adapters, N content, and low-quality bases. The processed reads, meeting all filtering criteria, were aligned to the human reference genome GRCh38 using BWA-MEM[28] (v0.7.17), resulting in the generation of BAM files. SAMtools[29] (v1.11) was then employed to sort and index the BAM files. Coverage analysis was conducted using SAMtools, and the mean coverage for the WGS data used in this study was determined to be 41X (Table S2).

Variant calling

SNVs and indels

Somatic mutations were detected from tumor samples, using matched germline samples as controls. In detail, somatic point mutations were detected using Mutect2[30] (v4.2.5.0). Somatic small indels were detected using Mutect2,[30] and Strelka2[31] (v2.9.10). Two software were run independently. The indels detected by two callers were merged using BEDTools (v2.30.0). The combined variant

format files (VCF) files were split and left trimmed using GATK (v4.2.5.0). The VCF was annotated using ANNOVAR.[32] To remove artifacts and false positives, we filtered for variants with > 0.01 allele frequency in 1000 Genomes or Exome Aggregation Consortium (ExAC)[33] unless ClinVar[34] flags it as pathogenic.

SVs

Somatic SVs were identified from paired tumor-germline WGS data using four callers: Delly2[35] (v1.1.3), SvABA[36] (v 1.1.0), Lumpy[37] (v0.2.13), and Manta[38] (v1.6.0). Each algorithm was executed independently. The SVs generated by each caller were merged using SURVIVOR[39] (v1.0.7), with a 1 Kb allowance for slop at the breakpoints. Only calls generated by at least two algorithms were retained. We calculated the number of SV for each sample.

CNVs

Tumor purity and ploidy were computed for all tumor and urine samples using FACETS[40] (v0.5.14). FACETS provides allele-specific estimations of the copy numbers. As previously described,[41] if the fraction of the genome with a major copy number ≥ 2 was greater than 50%, samples were classified as exhibiting whole genome duplication (WGD). Somatic CNVs were inferred by CNVkit[42] (v0.9.9). GISTIC2[43] was applied to evaluate the gene copy number status. The somatic variations (including CNV, SNV, and indel) in ten 10 canonical signaling pathways were assessed using maftools[44] (2.14.0).

Kataegis detection

We used maftools (v2.14.0)[44] to identify kataegis by analyzing mutation clusters across the genome.

Chromothripsis calling

Chromothripsis events were identified through ShatterSeek[11] (v1.1) using CNV and SV data as input. These chromothripsis events were classified into high-confidence (HC) and low-confidence (LC) categories based on established criteria outlined by Cortés-Ciriano et al. LC calls encompassed 4-6 segments between two states, while HC calls consisted of a minimum of 7 adjacent segments. Both HC and LC calls were retained for subsequent analysis. Moreover, we defined chromothripsis events in which more than 60% of the CN segments in the affected region oscillated between two states as canonical chromothripsis events.

Focal amplifications calling

To identify the presence of focal amplifications, we applied the AmpliconSuite-pipeline wrapper as previously described.[45] For seed detection, the wrapper pipeline integrated CNVKit[42] in tumor-normal mode, calling somatic CNVs against matched germline WGS data for each case. The amplified_intervals.py script was then utilized to filter regions with a copy number exceeding 4.5 and a size larger than 50 Kb, yielding a set of seed regions. Subsequently, the wrapper invoked AmpliconArchitect[20] (v1.3.r6) in default mode on the WGS BAM files to scrutinize seed regions and profile the architecture of focal amplifications. AmpliconClassifier[46] (v0.4.12) was used to predict the types of amplifications present in AmpliconArchitect's output. Through this approach, we categorized focal amplifications into ecDNA, BFB, and other fSCNA (including complex non-cyclic and linear focal amplifications).

Mutational signature analysis

Point mutations, including non-synonymous and synonymous mutations, were classified into 96 substitution types, based on six base substitutions (C > A, C > G, C > T, T > A, T > C, and T > G) and their neighboring bases. The MutationalPatterns[47] R package was employed to assess the activity of APOBEC-related mutational signatures (COSMIC SBS2 and SBS13) for each sample.

CNV signature quantification

The activities of the CNV signature were quantified using sigminer (v2.2.0) software.

Processing of RNA-seq data

The raw RNA-seq data from 328 tumors were evaluated for quality using FastQC (v. 0.11.7). We then used TrimGalore (v.0.6.7) to remove low-quality bases and adapter sequences. The clean reads were aligned to the human reference genome (GRCh38) using STAR[48] (v.2.7.10a). Transcript quantification was calculated using RSEM[49] (v.1.3.3). We filtered out genes with no expression in all of the samples for downstream GSVA analysis. Single-sample gene set enrichment analysis scores for each sample were calculated using the previously defined gene sets and the GSVA (v.1.46.0)[50] R package. DEG analysis was performed by DESeq2 (v.1.40.2).[51] ClusterProfiler (v.4.6.2)[52] R package was performed for KEGG pathway analysis.

Interphase FISH

Interphase FISH was carried out using the ZytoLight ® SPEC CCND1/CEN 11 Dual Color Probe to confirm CCND1 amplification in four available FFPE tumor samples. Briefly, FFPE samples were deparaffinized, rehydrated, and underwent heat-induced epitope retrieval. Slides were dehydrated, and FISH probes in a hybridization buffer were applied. Denaturation occurred at 72°C for 5 minutes, followed by overnight hybridization at 37°C. Slides were washed in 2×SSC/0.3% NP-40 (pH 7.0-7.5) and stained with 10μl of DAPI buffer. Images were captured using OLYMPUS BX53.

Analysis of clinical outcomes

The prognostic values of chromothripsis were assessed in our cohort. The sample size was $N = 436$ (272 chromothripsis^{+}; 164 chromothripsis^{-}). We employed the log-rank test to evaluate survival differences and conducted Cox proportional hazards regression analysis to identify independent prognostic factors. Survival curves were generated using the R package Survminer (v.0.4.9).

QUANTIFICATION AND STATISTICAL ANALYSIS

All statistical tests were performed in R (v4.2.2). Statistical tests, test statistics, and p values are indicated in figure legends and the results section. p-values < 0.05 were considered statistically significant.